PAPER

NJC
www.rsc.org/njc

The crossed interdiffusion of sodium nitrate and sulfate through an anion exchange membrane, as studied by Raman spectroscopy

Patrice Huguet,*[a] Timofei Kiva,[b] Olivier Noguera,[a] Philippe Sistat[a] and Victor Nikonenko[b]

[a] *Institut Européen des Membranes (CNRS UMR 5635), Université de Montpellier II CC047, Place Eugène Bataillon, 34095 Montpellier Cedex 5, France. E-mail: patrice.huguet@iemm.univ-montp2.fr; Fax: 33 (0)4 67 14 91 19; Tel: 33 (0)4 67 14 91 14*

[b] *Membrane Institute, Kuban State University, 149 Stavropolskaya st., 350040 Krasnodar, Russia. E-mail: v_nikonenko@mail.ru; Fax: 00 7 86 12 19 95 17; Tel: 00 7 86 12 19 95 73*

Received (in Montpellier, France) 25th January 2005, Accepted 18th March 2005
First published as an Advance Article on the web 9th June 2005

Raman spectroscopy is applied to visualize concentration profiles in solution adjacent to the top of DSV anion exchange membranes in horizontal positions. The concentration profiles of sulfates, nitrates and their fluxes through the membrane are recorded as a function of time during 13–15 h experiments. A three layer mathematical model based on extended Nernst–Planck equations with a convective term is developed. The membrane's kinetic and static parameters, such as ionic diffusion and ion exchange coefficients, are determined by separate experiments. Only one parameter, the diffusion boundary layer thickness, δ, is fitted. It is found that the model described fluxes well, especially when the variation of δ is taken into account. At the same time, the model gives nearly linear concentration profiles, whereas the measured profiles are much more complicated. This complicated shape is explained by natural convection and the emergence of the Bènard vortexes in the system.

Introduction

Ion transfer in solution boundary layers adjacent to membranes strongly affects their overall transport characteristics. The diffusion boundary layers (DBL) not only restrict the rate of membrane processes[1] such as dialysis or electrodialysis, but also change the permselectivity of membranes,[2] including their specific selectivity towards different kinds of ions.[3] Knowledge of the role of the DBL in the transport processes of systems is important for artificial, as well as biological[4,5] membranes. In the case of electrodialysis, the cause of ion concentration variation in the DBL is the difference between ion transport numbers in the solution and membrane.[1] In the case of dialysis where no current is applied, the driving force is the drop in chemical potential between the two solutions separated by the membrane. The concentration profiles arising in the membrane and DBL depend on the ionic mobility in both the membrane and solution, as well as the hydrodynamic conditions. Helfferich[1] has introduced a criterion that permits the determination of whether the membrane or the diffusion layer controls the self diffusion transfer rate. If the ratio $D_i c_i d : D_i^* c_i^* \delta \gg 2$, the rate is membrane-diffusion-controlled, and the diffusion flux density $J_i = D^*_i c^*_i / d$. In cases where $D_i c_i d : D_i^* c_i^* \delta \ll 2$ it is film-diffusion-controlled and $J_i = D_i c_i / \delta$. Here, D_i, c_i and J_i are the diffusion coefficient, ion concentration and ion flux density of ion "i" respectively. d and δ represent the thickness of the membrane and DBL respectively. The asterisk refers to the quantities in the membrane.

The visualisation of concentration profiles close to a membrane during a transfer process are of great interest because they allow a better understanding of the phenomena restricting processing rate. Clifton and Sanchez,[6] Shaposhnik *et al.*[7] and Dworecki *et al.*[8] have used non-destructive laser holography to visualise concentration profiles in DBL. However, the optical index variation, which is the basis of measurements, depends not only on the ion concentration, but also on temperature. An original method of visualisation proposed by Pérrez-Herranz *et al.*[9] was to use a dilute solution of an indicator; one that reacts with H^+ generated at the membrane surface when an electrodialysis cell operates above its limiting current density. The coloured trace of the indicator was filmed with a video camera. Antonenko and Pohl[5] have used pH microelectrodes for measuring the pH profile near to bilayer lipid membranes.

A way of evaluating the DBL thickness, δ, is to use electrochemical methods. Determination of the limiting current density, i_{lim}, and then applying the well known relationship between i_{lim} and δ[1] is the most common technique for obtaining the value of δ,[3,9] including the case of the rotating membrane disc developed by Bobreshova *et al.*[10] The advantage of this latter technique is that the diffusion layer thickness is uniform on the membrane surface and can be calculated using the rotation frequency. Sistat and Pourcelly[11] have developed a technique allowing the determination of δ from chronopotentiometric measurements. There are a number of other, less common, methods for studying the shape and the thickness of the boundary layer.[9]

Raman spectroscopy is a power technique for studying concentration profiles in transparent or translucent milieu because the spectra of their different constituents are easily acquired.[12,13] In this paper we apply the technique to measuring the concentration profiles in DBL near an anion exchange membrane during the interdiffusion of sodium nitrates and sulfates.

Experimental

Membrane

An anion exchange DSV membrane produced by Asahi Glass, Japan, Selemion was used in this study. The membrane has an organic microporous matrix containing strongly basic, positively charged sites; the principal application being Donnan

DOI: 10.1039/b501257k

Table 1 Electrical conductivity, κ, of DSV membrane, equilibrated with Na_2SO_4 and $NaNO_3$ solutions of various concentrations

C/mol L^{-1}	Na_2SO_4 κ/S m^{-1}	$NaNO_3$ κ/S m^{-1}
0.05	0.592	0.797
0.1	0.721	0.782
0.3	0.744	0.939
0.5	0.908	1.006
1.0	0.913	1.143

dialysis. The main properties of the membrane are (1) the ion exchange capacity of dry membrane is 2.05 mequiv. g^{-1}, corresponding to 1.53 mequiv. cm^{-3} of wet membrane, (2) its saturated water content falls in the range 0.32–0.40 g_{H_2O} $g^{-1}_{wet\ membrane}$, (3) the wet membrane density is ~1.1 g cm^{-3} and (4) its thickness is 150 μm.

Cell

The cell used in our experiments had two circular compartments, divided by the membrane being studied. The membrane active area was 18.1 cm^2. The solution volume was 25 mL in the upper compartment, and 33 mL in the lower. Part of the solution in both compartments stayed in the tubes used to fill each compartment with solution. The volume of this "dead" solution (because it does not take part in the ion exchange) was ~8 mL for the lower compartment and 4–6 mL for the upper.

1 M $NaNO_3$ and Na_2SO_4 solutions were used to fill the upper and the lower compartments respectively. The upper solution was analysed by the laser beam of a confocal Raman spectrometer. Both solutions were analysed by the Raman spectroscopy and photometry at the end of each 12–14 h experiment.

Membrane characterisation

In order to better understand the behaviour of the membrane during interdiffusion, and to use its parameters in modelling, a number of membrane properties were measured. Electrical conductivity was measured by the impedance method with a mercury cell[14–18] (Table 1). Diffusion and osmotic permeability were measured using a 1 M $NaNO_3$ solution filling one of the cell compartments (initial volume 30 mL) and pure water (initial volume 29 mL) filling the other (Table 2), the membrane area was 4.52 cm^2. All measurements were carried out at 25 ± 0.5 °C.

Results

Electrical conductivity and electrolyte sorption

Treatment of the conductivity data in log κ–log C coordinates allows the following interpolations to be obtained for the Na_2SO_4 and $NaNO_3$ solutions respectively: $\log \kappa = 0.1414 \log C - 0.0275$ and $\log \kappa = 0.1283 \log C + 0.0457$. In accordance with the microheterogeneous model,[19–21] the proportionality coefficient at log C has the sense of volume fraction of the electroneutral intergel solution (f_2) in the membrane. This solution fills the central regions of the macro- and mesopores as well as the caverns and cavities, if they exist, in the membrane. Hence in two cases, the values of the f_2 parameter are close (~0.13). This value characterises the DSV membrane as a porous medium. In comparison, the f_2 for the homogeneous MF-4SK membrane is between 0.01–0.05;[19,20] for heterogeneous membranes such as MK-40, the MA-40 parameter is close to 0.2.[19,20]

The amount of an electrolyte sorbed by a membrane (*i.e.* removable by a sufficiently large amount of water) may be presented as the sum of the electrolyte sorbed by the gel regions and by the electroneutral "intergel" solution. The gel regions are relatively homogeneous, microporous parts of the membrane, containing both fixed and mobile ions, as well as water molecules and polymer chains. Thus, the concentration of sorbed electrolyte, c^*_E, can be presented as follows:[19]

$$c^*_E = f_1 \bar{c}_E + f_2 c_E \quad (1)$$

where f_1 and f_2 are the volume fractions of the gel regions ($f_1 + f_2 = 1$), and $\bar{c}_E$ and c_E are the electrolyte concentrations in the gel and "intergel" regions respectively, the former supposedly being the same as that of the equilibrium external solution. As the DSV membrane has a relatively high ion exchange capacity and a high volume fraction of "intergel" spaces filled with the electroneutral solution (f_2), the contribution of the gel regions to the electrolyte sorption should be small.[19,22] For approximate calculations of c^*_E, it is therefore possible to neglect the first term in eqn. (1) and write:

$$c^*_E \approx f_2 c_E \quad (2)$$

The total counterion concentration in the membrane is found in a similar way to that of the co-ion:

$$c^*_1 = f_1(\bar{Q}/z_1) + f_2 c_1 \quad (3)$$

where z_1 is the charge number of the counterion and $\bar{Q}/z_1^{-1}$ is its molar concentration in the gel phase; $\bar{Q}$ being the concentration of fixed groups in the gel (/mequiv. cm^{-3}). Wet: $\bar{Q} = Q/f_1$.

Diffusion permeability

From the measurements of the $NaNO_3$ diffusion, the integral (global) permeability coefficient was determined: $P = J_E d/c_E \approx 6.0 \times 10^{-7}$ cm^2 s^{-1}, where J_E is the electrolyte flux density through the membrane and d is its thickness ($c_E = 1$ mol L^{-1}). The local diffusion permeability, P^*, is defined as:

$$P^* = -\frac{J_E}{dc/dx} \quad (4)$$

and can be calculated from P if the concentration dependence $P(c_E)$ is known:[20,21,23]

$$P^* = P + c_E \frac{dP}{dc_E} \quad (5)$$

Table 2 Variation in the nitrate concentration and the solution volume in two compartments of a cell initially filled with 1 M $NaNO_3$ and pure water

t/h	t/s	Nitrate concentration in the 1st compartment, C/mol L^{-1}	Nitrate concentration in the 2nd compartment, C/mol L^{-1}	Volume variation in the 1st compartment, V/mL	Volume variation in the 2nd compartment, V/mL
0	0	1	0	0	0
Run 1					
3	10 800			0.1	−0.1
6	21 600			0.2	−0.2
7.75	27 900	0.85	0.15	0.22	−0.22
Run 2					
14	50 400	0.81	0.22	0.37	−0.37

As the determination of P as function of c_E is laborious, an approximate evaluation of P^*, without measurement of $P(c_E)$, is sufficient for the calculations in this paper. It is known[23] that $\frac{dP}{dc_E}$ is usually positive and that P^* is 1.3–1.4 times higher than P in the case of an ion exchange membrane characterised by a relatively high f_2 value. Hence the value $P^* = 8.6 \times 10^{-7}$ cm^2 s^{-1} was taken in the case of the $NaNO_3$ solution.

Diffusion coefficients in the membrane

When introducing effective diffusion coefficients D_i^* for ions "i" in the membrane, the electrical conductivity κ^* and the local diffusion permeability P^* can be expressed as:[19]

$$\kappa^* = \frac{F^2}{RT}(z_+^2 D_+^* c_+^* + z_-^2 D_-^* c_-^*) \quad (6)$$

$$P^* = (z_+ D_+^* c_+^* t_-^* \quad + \quad |z_-| D_-^* c_-^* t_+^*)/|z_i| c_i \quad (7)$$

where:

$$t_i^* = z_i^2 D_i^* c_i^*/(z_+^2 D_+^* c_+^* \quad + \quad z_-^2 D_-^* c_-^*) \quad (8)$$

is the transport number of ion "i". The indices "+" and "−" refer to the cation and anion respectively.

By using the measured values of κ^* for 1 M $NaNO_3$ and 1 M $NaSO_4$, approximations (eqn. (2)) for sorbed electrolyte concentrations, and the P^* value estimated for 1 M $NaNO_3$, we find that the diffusion coefficients for NO_3^-, SO_4^{2-} and Na^+ ions in the membrane are 1.5, 0.56 and 4.0 ($\times 10^{-6}$ cm^2 s^{-1}) respectively. The transport numbers found in the DSV membrane, equilibrated with 1 M solution of the corresponding salt, in this case are 0.83 and 0.79 for NO_3^- and SO_4^{2-} anions respectively. The P^* value for the DSV membrane equilibrated with 1 M Na_2SO_4 solution is 6.2×10^{-7} cm^2 s^{-1}.

Filtration permeability

The filtration permeability coefficient ($L_p = 7.5 \times 10^{-9}$ cm^5 J^{-1} s^{-1}) can be determined from the variation of the volume (ΔV) in the upper and lower compartments as a function of time. $\Delta V = 0.1$, 0.2, 0.22 and 0.32 mL respectively after 3, 6, 7.75 and 14 h from the start of the experiment.

Ion exchange coefficient

To find the ion exchange coefficient necessary for mathematical modelling, an evaluation of the exchange of sulfates and nitrate ions of sodium with a total Na^+ concentration of 1 M was carried out. The results are presented in Table 3.

The following equation was used to describe the experimental data:

$$\frac{(c_{SO_4}^*)^{1/2}}{c_{NO_3}^*} = K_{NO_3}^{SO_4} \frac{(c_{SO_4})^{1/2}}{c_{NO_3}} \quad (9)$$

The ion exchange coefficient $K_{NO_3}^{SO_4}$ was found to be 0.17.

Raman measurements

Raman measurements were performed using a confocal Raman microprobe system (LabRam 1B from HORIBA DILOR, France). Excitation at $\lambda = 632.818$ nm was provided by a He–Ne laser, and the power delivered was ~17 mW (~12 mW at sample). A long working distance Olympus objective (×50, 0.50 numerical aperture) was used to perform the experiments. The hole aperture of the confocal diaphragm was set to 900 μm. Confocality tests on a reference Si wafer showed a spatial resolution along the optical axis of 22 μm.

The results of the crossed interdiffusion experiments are presented in Fig. 1, Table 4 and Table 5.

Table 3 Results of equilibrium ion exchange measurements

Equivalent fraction SO_4^{2-} in the solution	0	0.2	0.4	0.6	0.8	1
Equivalent fraction SO_4^{2-} in the membrane	0	0.0366	0.0453	0.618	0.885	1

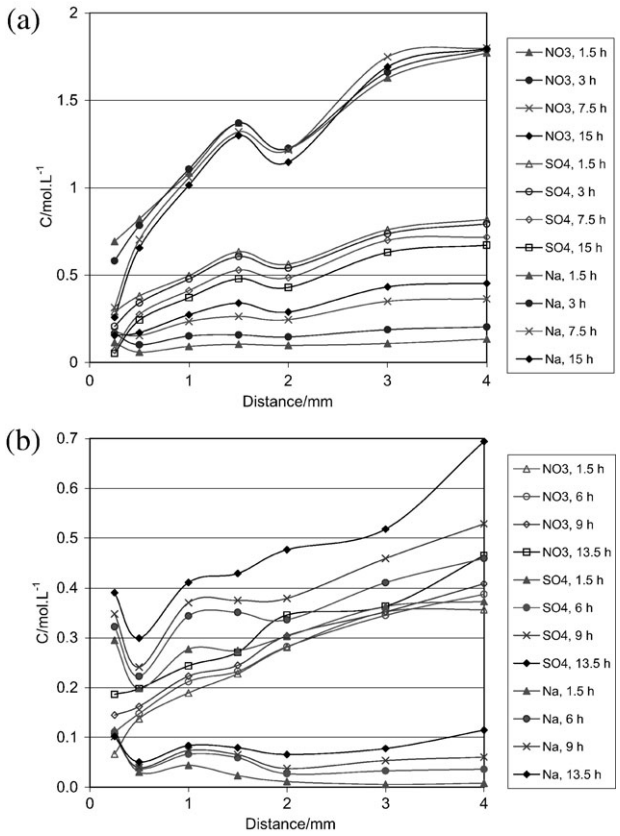

Fig. 1 Concentration profiles above an anion exchange DSV membrane, obtained by Raman spectroscopy in solution, during crossed interdiffusion of Na_2SO_4 and $NaNO_3$ for the cases where sulfates (a) and nitrates (b) were initially in the upper compartment.

Model

The membrane system is considered as a plane, five layer system, including the membrane under investigation, two DBLs adjacent to the membrane and two bulks, where the concentration distribution is uniform but can change with time (Fig. 2). The transport of ion species "i" in the DBL and the membrane is described by the extended Nernst–Planck equation, containing a convective term:

$$J_i = -D_i\left(\frac{dc_i}{dx} + z_i c_i \frac{F}{RT}\frac{d\varphi}{dx}\right) + (1-\sigma)c_i J_v \quad (10)$$

where D_i is the ionic diffusion coefficient, φ the electric potential, J_v the volume flux, and R, T and F have their usual meanings. σ is the Staverman reflection coefficient of the membrane. When $\sigma = 1$, the membrane is not permeable by the electrolyte (total reflection) and when $\sigma = 0$, the transport takes place in the solution. As the current is zero, the fluxes are linked by the equation:

$$\sum_i z_i J_i = 0 \quad (11)$$

The concentrations, c_i, satisfy the electroneutrality equation:

$$\sum_i z_i c_i = 0 \quad \text{in the solution} \quad (12)$$

Table 4 Average concentrations in the compartments, obtained by Raman spectroscopy, at the end of the experiment ($t = 15$ h), sulfates initially being in the upper compartment

	Upper compartment, $V_{ini} = 25$ mL			Lower compartment, $V_{ini} = 33$ mL		
Experiment number	C (sulfates)/ mol L^{-1}	C (nitrates)/ mol L^{-1}	C (sodium)/ mol L^{-1}	C (sulfates)/ mol L^{-1}	C (nitrates)/ mol L^{-1}	C (sodium)/ mol L^{-1}
1[a]	0.64	0.45	1.73	0.21	0.61	1.02
2[a]	0.62	0.43	1.68	0.21	0.57	0.99
3[a]	0.71	0.36	1.78	0.19	0.61	0.99
4[a]	0.85	0.34	2.04	0.16	0.64	0.96
5[a]	0.63	0.41	1.67	0.15	0.59	0.89
Average	0.63	0.40	1.78	0.184	0.60	0.97
Average[b]	0.73	0.37	1.83	0.17	0.61	0.95
Average[c]	0.66	0.49	1.81	0.17	0.71	1.04
For calculated values:						
Calculated[d]	0.721	0.330	1.779	0.20	0.745	1.157
Calculated[e]	0.723	0.389	1.80	0.214	0.699	1.139

[a] Analysed by Raman spectroscopy. [b] Average data from experiments 3, 4 and 5, analysed by Raman spectroscopy. [c] Average data from experiments 3, 4 and 5, analysed by capillary electrophoresis. [d] δ is constant and equal to 2.2 mm. [e] δ is a function of time, presented in Fig. 4.

$$\sum_i z_i c_i^* = Q \quad \text{in the membrane} \tag{13}$$

In 3D cases for an incompressible fluid, the equation of continuity is written as:

$$div J_v = 0 \tag{14}$$

In the 1D case under consideration J_v is constant in the membrane and solution.

The volume flux density through the membrane is determined by the following equation, a particular case of the Kedem–Katchalsky equation,[23,24] where the sole moving force is the osmotic pressure gradient:

$$J_v = L_p \sigma \frac{\Delta\pi}{d} \approx L_p \sigma RT \frac{\Delta \sum_i c_i}{d} \tag{15}$$

where L_p is the previously discussed filtration permeability coefficient and $\Delta\pi$ or $\Delta\sum c_i$ denotes the difference in π or $\sum c_i$ function values respectively between the one side and the other side of the membrane.

The equation of material balance (1D case) is applied in the membrane and the two DBLs:

$$\frac{\partial c_i}{\partial t} = -\frac{\partial J_i}{\partial x} \tag{16}$$

At membrane–solution interfaces, continuity of the ionic and volume fluxes is assumed—the local thermodynamic equilibrium supposedly being held here. The concentrations of co-ion in the membrane and solution phases at the interfaces are linked by eqn. (2), and similarly counterions by eqn. (9).

The volume osmotic flux from the more dilute to the more concentrated solution will dilute the boundary solution layer of the more concentrated solution. We can suppose for simplicity that the membrane is characterised by $\sigma = 1$ (the membrane is not permeable by the electrolyte) and only convective flow occurs in the system (hence the diffusion and migration terms are zero in eqn. (10)), J_i entering the boundary concentrated solution layer is zero, whereas J_i residing in this layer is positive.

The bulk concentration, c_i^b, is calculated by balance, eqn. (17):

$$\frac{\partial}{\partial t}\left(c_i^b L^b + \int_0^\delta c_i \, dx\right) = \pm J_i^m \tag{17}$$

where L^b and δ are the thickness of the bulk solution and DBL (supposedly the same for the both sides of the membrane) respectively, and J_i^m is the flux density of ion "i" through the membrane–solution interface. The sign is "+" for the solution on one side and "−" for the solution on the other side. In general cases, L^b and δ vary with time, and the total thickness of the solution layer is:

$$L^b + \delta = L_0^b + \delta_0 + \int_0^t J_v \, dt \tag{18}$$

where L_0^b and δ_0 are the thickness of the bulk solution and DBL at $t = 0$ respectively.

The problem was numerically resolved by using a finite-difference method. All the space, including the two diffusion layers and the membrane, are divided into N segments, the length of segments being different for the membrane and

Table 5 Average concentration in the compartments at the end of the experiment ($t = 15$ h), obtained by Raman spectroscopy; the nitrates initially being in upper compartment

	Upper compartment, $V_{ini} = 25$ mL			Lower compartment, $V_{ini} = 33$ mL		
Experiment number	C (sulfates)/ mol L^{-1}	C (nitrates)/ mol L^{-1}	C (sodium)/ mol L^{-1}	C (sulfates)/ mol L^{-1}	C (nitrates)/ mol L^{-1}	C (sodium)/ mol $^{-1}$
1	0.22	0.82	1.27	0.90	0.25	2.05
2	0.23	0.83	1.28	0.73	0.21	1.67
3	0.19	0.64	1.02	0.74	0.20	1.68
4	0.19	0.71	1.09	0.84	0.23	1.91
5	0.20	0.74	1.13	0.88	0.21	1.97
Average[a]	0.21	0.75	1.16	0.82	0.22	1.85
Calculated values (constant $\delta = 4$ mm)						
	0.24	0.70	1.19	0.81	0.23	1.85

[a] Average data from all the experiments.

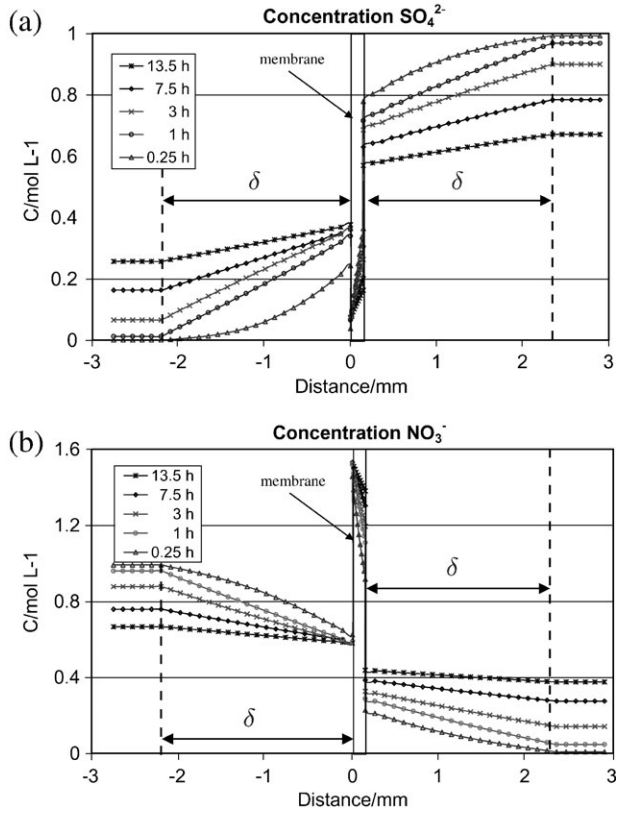

Fig. 2 Calculated concentration profiles of sulfates (a) and nitrates (b) for the case where sulfates were initially in the upper compartment. The point of origin is set on the left side of the membrane and δ is taken as a constant equal to 2.2 mm.

diffusion layers, in general cases. As the initial concentrations at $t = 0$ are known, the volume flux in each segment can be calculated from eqn. (15) and the ionic fluxes from eqn. (10), the electric field having previously been calculated from eqn. (11). Eqn. (16) then allows new concentrations at $t = \Delta t$ to be calculated, where Δt is the time step interval. This procedure is then repeated. The general method is similar to that described by Garrido *et al.*[25] The transition from boundary solution concentrations to that in the membrane and the inverse transition are made by simultaneously resolving eqn. (2), eqn. (9), eqn. (12) and eqn. (13).

The following parameter values were taken for calculations. The individual ionic diffusion coefficients in the solution were estimated for 1 M Na_2SO_4 and 1 M $NaNO_3$ by using the data of Robinson and Stokes:[26] $D_{Na} = 1.17$, $D_{NO_3} = 1.56$ and $D_{SO_4} = 0.53$ ($\times 10^{-5}$ cm^2 s^{-1}), taking into account that the diffusion coefficients of weakly hydrated ions (such as NO_3^-) change less with the concentration. The diffusion coefficients in the membrane were: $D^*_{Na} = 0.35$, $D^*_{NO_3} = 0.20$ and $D^*_{SO_4} = 0.056$ ($\times 10^{-5}$ cm^2 s^{-1}). The volume fraction of electroneutral solution in the membrane, f_2, was 0.13, as determined by membrane conductivity measurements of the different ionic forms, and sodium nitrate diffusion. The ion exchange equilibrium coefficient, $K^{SO_4}_{NO_3}$, was resolved to be 0.17 from corresponding experiments. The filtration coefficient (L_p) value of 7.5×10^{-9} cm^5 J^{-1} s^{-1} was determined from the variation of the solution volume during sodium nitrate diffusion. It is important to note that L_p has little influence on the calculation results if it maintains the same order of magnitude. Only one parameter was fitted—the effective thickness of the diffusion layer, δ, considered to be the same at both membrane surfaces.

Discussion

It is easy to evaluate the Helfferich criterion described in the Introduction. When taking values in the order of 10^{-5} and 10^{-6} cm^2 s^{-1} for the diffusion coefficient in the solution and the membrane respectively, 1 mol L^{-1} for the concentration in both phases, and 150 and 2000 μm for the thickness of the membrane and the diffusion layer respectively, we find this criterion to be ~1. Hence the kinetics type is controlled by diffusion in both the membrane and diffusion layers.

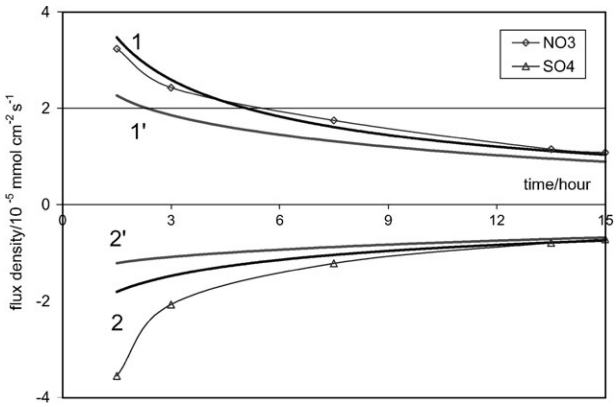

Fig. 3 Time-averaged fluxes of sulfates and nitrates through an anion exchange DSV membrane *vs.* time in the case where sulfates were initially in the upper compartment. Points are experimental values. Curves are calculated at variable time (1 and 2) and constant δ value (1′and 2′).

Two types of calculations were performed—either assuming a constant δ value or variable time. A constant value of δ was fitted for the average concentrations in both compartments at the end of measurements ($t = 15$ h), averaged over several experiments. Values for δ of 2.2 mm and 4 mm respectively were found in the cases where the sulfates and nitrates initially started in the upper compartment. Fig. 1a and 1b show that the values of δ correspond approximately to the distance between the membrane and the intersection of tangents drawn in the concentration profile near the interface and in the bulk. The results of the calculations presented in Table 4 and Table 5 correlate well with the experimental data concerning the average concentrations in each compartment at the end of the interdiffusion experiments. As there is no forced convection, the diffusion boundary layer is formed under the action of natural gravitational convection, the driving force being the solution density vertical gradient. The difference in δ for the two considered cases is explained by the fact that the sodium sulfate solution is more concentrated. If all species are taken into account $c_{Na} = 2$ mol L^{-1}. In the case of sulfates initially in the upper compartment, a more diluted, and hence lighter boundary solution layer appears near the upper side of the membrane (the bottom of the compartment), the heavier layer being at the top of this compartment.

Fig. 3 shows the time-averaged fluxes through the membrane *vs.* time, in the case where the sulfates were initially in the upper compartment. The experimental values are obtained by graphical integration of the measured concentration profiles and the application of an integral balance equation that takes the form:

$$V_{av}(t)\Delta c_i(t) = SJ_{avi}(t)t \qquad (19)$$

where $V_{av}(t)$ and $J_{avi}(t)$ are the time-averaged volume of the upper compartment and the flux density of species "i" respectively, $\Delta c_i(t)$ is the increment in average concentration over time t, and S is the surface area of the membrane. If the diffusion layer thickness is presumed to be constant, the calculated average flux density is lower than that determined experimentally at the beginning of the interdiffusion. To obtain higher fluxes, lower values of δ should be assumed at shorter interdiffusion times. Fig. 4 presents the values of δ as function of time, the use of which gives stronger agreement between calculated and experimental time-averaged flux densities. The increase in values of δ with time is explained by the action of

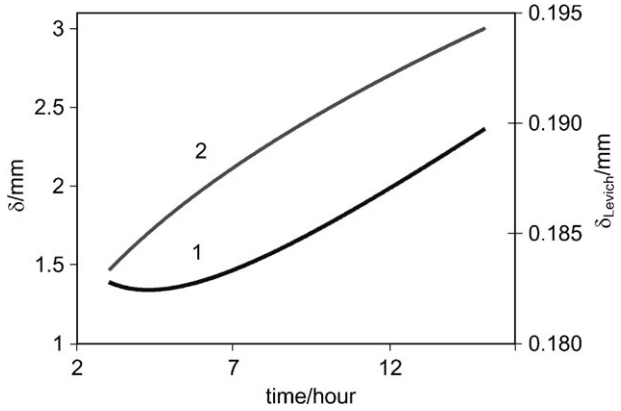

Fig. 4 Diffusion boundary layer thickness as a function of time calculated using Levich's eqn. (20) (curve 1), and obtained by fitting the experimental fluxes (presented in Fig. 3) with the model (curve 2).

two factors. Firstly, at the beginning of the interdiffusion δ is zero and then increases with time. Secondly, when the interdiffusion becomes a quasi steady state, the main reason is that the decrease in the concentration difference between the boundary and bulk values with time results in a decrease in the solution density gradient—the driving force of gravitational convection.

In the considered cases, the membrane was horizontal. A number of vortexes, forming so-called Bènard's cells, also appear[27–29] in the course of the gravitational convection. The calculation of δ is rather difficult in these cases. However, it is possible to calculate δ for the case of a vertical membrane position by using the Levich equation:[28]

$$\delta \approx \frac{x^{1/4}}{0.7Pr^{1/4}\left(\frac{g(c^{b}-c^{s})}{4\nu^{2}}\right)^{1/4}} \qquad (20)$$

where x is the height of the membrane, g the gravitational acceleration, ν the electrolyte viscosity, $(c^{b} - c^{s})$ the difference in bulk and interfacial electrolyte concentration in g cm^{-3} and $Pr = \nu D^{-1}$, where D is the electrolyte diffusion coefficient.

Fig. 4 presents, together with δ determined from experimental data by using the described model, the results of the calculation of δ using eqn. (20). The distance x was taken to be the radius of the membrane (2.4 cm), $Pr = 1250$ and $D_{Na_2SO_4} = 0.8 \times 10^{-5}$ cm^2 s^{-1}. As Fig. 4 shows, the δ values calculated for vertical positions are significantly lower than those determined experimentally with the interdiffusion through a horizontal membrane, in accordance with the theory of physicochemical hydrodynamics.[27–29] The tendency of δ to increase with time is observed in both cases and occurs because of a decrease in $(c^{b}_{Na} - c^{s}_{Na})$. However, δ_{Levich} passes through a minimum. This is explained by the fact that eqn. (20) gives a stationary value that supposes δ does not change with time for a given concentration difference. Hence, small values of $(c^{b}_{Na} - c^{s}_{Na})$ at the beginning suppose high values of δ_{Levich}.

The fact of a good agreement is found between calculated and measured ionic fluxes through the membrane is evidence that the Nernst concept of a stagnant diffusion layer serves as a good model for these purposes. At the same time, the shape of the calculated and measured concentration profiles are quite different—nearly linear as calculated and significantly more complicated as measured. This complicated shape may be explained by natural convection and emergence of Bènard vortexes in the system.

Natural convection produced by gravitational forces is characterized by the Rayleigh number (Ra):[27–29]

$$Ra = \frac{\Delta\rho}{\rho}\frac{gh^{3}}{\nu D} \qquad (21)$$

where $\Delta\rho$ is the solution density drop across the layer where the density, ρ, varies and h is the thickness of this layer. In the case of a horizontal membrane position, gravitational convection can occur when a lighter solution layer is below a heavier one and Ra is higher than its critical value ($Ra_c = 1708$). Convection occurs when the density of a small volume of solution decreases accidentally due to a fluctuation, and the volume is lifted due to the Archimedes force. If $Ra < 1708$, the diffusion relaxation time is higher than the time needed for lifting of the considered volume and the fluctuation disperses faster than the volume changes its position considerably. If $Ra > 1708$, the lifting rate of the volume is sufficiently high and the volume acquires solution layers of a higher density more rapidly than its own density becomes equal to that of the environment. As Fig. 2a shows, in the case of the sodium sulfate being initially in upper compartment, the characteristic concentration drop near the membrane is about 0.5 M Na_2SO_4, and the distance where this variation occurs is about 3 mm. The corresponding drop in the solution density is about $\Delta\rho = 0.06$ g cm^{-3}. Considering the order of magnitudes of ν ($\sim 10^{-2}$ cm^2 s^{-1}) and D ($\sim 10^{-5}$ cm^2 s^{-1}), we find that $Ra \sim 10^7$—much higher than the critical value. As was mentioned above, the experience shows a clear difference between the DBL thickness was found between the cases where the sodium sulfate and the sodium nitrate were initially in the upper compartment. Hence, a heavier solution layer was placed on the top of a lighter one in the former case, and the reciprocal scenario was presented in the latter. Following the theory, in the second case, no convection should be produced. However, a concentration boundary layer was observed. This could be explained by a possible small deviation of the system from a true horizontal position coupled with a Ra number that was evidently sufficiently high to yield convection.

Volgin *et al.*[30] have proposed a mathematical model of gravitational convection in the solution between two parallel horizontal plates. They have shown that the solution density increases in the vertical direction and $Ra > Ra_c$, the vortexes of approximately square shape with the same size as the thickness of the liquid layer appear. Two neighbouring vortexes turn in opposite directions in such a way that the solution between them goes either up (lighter, less concentrated) or down (heavier, more concentrated). The shape of the concentration distribution looks like two mushrooms in which the cap will be represented by the lifting lighter solution, and the foot by the descending heavier solution. When a small volume of lighter solution goes up, and if the exchange of matter is not too fast between this volume and surrounding solution, then a volume with a less concentrated solution may appear higher. Hence, minima and maxima on the concentration profile drawn on the vertical axis can appear. Similar results were obtained by modelling convective diffusion, caused by concentration polarisation in a membrane system under a direct current passage, the membranes being in vertical position, a weak forced solution flowing imposed.[31] In this case local maxima and minima on the concentration profile appear in the latter half of the cell (if the beginning is at the solution entrance).

Conclusion

A Raman spectroscopy study of the interdiffusion of sulfates and nitrates through an anion exchange membrane (DSV) in a horizontal position, without force convection, revealed complicated concentration profiles, with local minima and maxima appearing in the upper cell compartment. A three layer mathematical model based on the Nernst–Planck transport equations allowed the calculation of ionic fluxes through the membrane. Concentration profiles of the thickness of the diffusion boundary layer (δ) were set as parameters. Partial film kinetics took place in the systems where comparable concentration gradients appeared in both the membrane and the two diffusion layers. It was found that δ varied with time,

being about 2 and 4 mm respectively in the cases where 1 M sodium sulfate and 1 M sodium nitrate solutions were initially in the upper cell compartment. The differences in δ could be explained by the fact that in the first case, a heavier solution layer (of Na_2SO_4) was placed above a lighter one (of $NaNO_3$); the situation being reversed in the second case. The value of δ was about 10 times higher compared to that calculated by the Levich equation for vertical positioning of the membranes. δ increased with time, following the decrease in electrolyte concentration drop across the boundary layer.

A good agreement between calculated and measured ionic fluxes through the membrane was found. This is evidence that the Nernst concept of a stagnant diffusion layer is a good model for flux calculations. At the same time, the model gave near-linear concentration profiles, whereas the measured ones were much more complicated. This complicated shape was explained by natural convection and the emergence of the Bènard vortexes in the system.

Acknowledgements

V.N. thanks the Institut Européen des Membranes for providing the opportunity to undertake the research described in this publication. This research was also financially supported by the CNRS, France, grant PICS No 1811, by INTAS-Kazakhstan project 04-81-7318 and by the Russian Foundation of Basic Researches, grant No 03-03-96571.

References

1 F. Helfferich, *Ion Exchange*, McGraw-Hill, New York, 1962.
2 J.-P. Hsu, K.-L. Yang and K.-C. Ting, *J. Phys. Chem. B*, 1997, **101**(44), 8984.
3 A. B. Yaroslavtsev, V. V. Nikonenko and V. I. Zabolotsky, *Chem. Rev*., 2003, **72**(5), 438.
4 V. V. Nikonenko, V. I. Zabolotsky and K. A. Lebedev, *Elektrokhimiya*, 1996, **32**, 258.
5 Yu. N. Antonenko and P. Pohl, *Biochim. Biophys. Acta*, 1995, **1235**, 57.
6 V. Sanchez and M. Clifton, *J. Chem. Phys*., 1980, **77**, 421.
7 V. A. Shaposhnik, V. I. Vasileva and D. Praslov, *J. Membr. Sci*., 1995, **101**, 23.
8 K. Dworecki, S. Wasik and A. Slezak, *Physica A (Amsterdam)*, 2003, **326**, 360.
9 V. Pérrez-Herranz, J. L. Guinon and J. Garcia-Anton, *J. Appl. Electrochem*., 2000, **30**, 809.
10 O. V. Bobreshova, P. I. Kulintsov and E. M. Balavadze, *J. Membr. Sci*., 1995, **101**, 1.
11 P. Sistat and G. Pourcelly, *J. Membr. Sci*., 1997, **123**, 121.
12 M. E. Vallejo, P. Huguet, C. Innocent, F. Persin, J. L. Bribes and G. Pourcelly, *J. Phys. Chem. B*, 1999, **103**, 11366.
13 M. Chaouki, P. Huguet, F. Persin and J. L. Bribes, *New J. Chem*., 1998, **3**, 233.
14 C. Gavach, G. Pamboutzoglou, M. Nedyalkov and G. Pourcelly, *J. Membr. Sci*., 1989, **45**, 37.
15 A. I. Meshechkov, O. A. Demina and N. P. Gnusin, *Elektrokhimiya*, 1987, **23**, 1452.
16 G. Pourcelly, A. Oikinomou, C. Gavach and H. D. Hurwitz, *J. Electroanal. Chem*., 1990, **287**, 43.
17 Yu. M. Vol'fkovich, N. S. Khoszyainova, V. V. Elkin, N. P. Berezina, O. P. Ivina and V. M. Mazin, *Elektrokhimiya*, 1988, **24**, 344.
18 P. Sistat, Thesis, *Apports des techniques électriques de relaxation à la compréhension des phénomènes de transport de matière dans un système membrane ionique-solution*, Université de Montpellier II, 1997.
19 V. I. Zabolotsky and V. V. Nikonenko, *J. Membr. Sci*., 1993, **79**, 181.
20 V. I. Zabolotsky and V. I. Nikonenko, *Ion Transport in Membranes*, Nauka, Moscow, 1996.
21 N. P. Gnusin, N. P. Berezina, O. A. Demina and N. A. Kononenko, *Russ. J. Electrochem*., 1996, **32**, 154.
22 V. I. Zabolotsky, V. V. Nikonenko, O. N. Kostenko and L. F. Elnikova, *Zh. Fiz. Khim*., 1993, **67**, 2423–2427.
23 B. Auclair, V. Nikonenko, C. Larchet, M. Métayer and L. Dammak, *J. Membr. Sci*., 2002, **195**, 89.
24 O. Kedem and A. Katchalsky, *Trans. Faraday Soc*., 1963, **59**, 1918.
25 J. Garrido, S. Mafé and J. Pellicer, *J. Membr. Sci*., 1985, **24**, 7.
26 R. A. Robinson and R. H. Stokes, *Electrolyte Solutions*, Butterworth, London, 2nd edn., 1959, pp. 513–515.
27 E. Guyon, J.-P. Hulin and L. Petit, *Hydrodynamique PhysiqueMatière Condensée Savoirs Actuels*, InterEditions, Paris, 2001.
28 V. G. Levich, *Physicochemical Hydrodynamics*, Prentice-Hall, New York, 1962, pp. 134.
29 A. P. Grigin and A. D. Davydov, *Elektrokhimiya*, 1998, **34**, 1237.
30 V. M. Volgin, O. V. Volgina, D. A. Bograchev and A. D. Davydov, *J. Electroanal. Chem*., 2003, **546**, 15.
31 A. Pismenskiy, M. Urtenov, V. Nikonenko, N. Pismenskaya and G. Pourcelly, presented at *Euromembrane 2004, 28 September–1 October*, Hamburg, Germany, 2004, pp. 489.